Numerical study on triggering of neoclassical tearing modes by sawteeth

Q. Yu, S. Günter and K. Lackner

Max-Planck-Institut für Plasmaphysik, 85748 Garching, Germany

1. Introduction

Sawtooth is an ubiquitous phenomenon in tokamaks, which among other deleterious effects can also trigger neoclassical tearing modes (NTMs) for a sufficiently high plasma beta value in experiments [e.g. 1-4]. The onset of NTMs usually significantly degrades plasma confinement or even leads to plasma major disruption. Understanding of the physics involved in the triggering of NTMs by sawteeth remains an important issue for a fusion reactor.

In this paper, this issue is studied numerically using the following normalized four-field equations, including the electron continuity equation, generalized Ohm's law and the equation of motion in the perpendicular (after taking $\mathbf{e}_t\cdot\nabla\times$) and the parallel direction,

$$\frac{dn_e}{dt} = d_1(\nabla_\parallel j - \varepsilon\beta_e \frac{\partial(n_e + \phi/\Omega)}{\partial z}) - \nabla_\parallel(n_e v_\parallel) + \nabla\cdot(D_\perp \nabla n_e) + S_n \quad (1)$$

$$\frac{d\psi}{dt} = E_0 - \eta\,(j - j_b) - \frac{\eta}{\nu_{ei}}\frac{dj}{dt} + \eta\frac{\mu_e}{\nu_{ei}}\nabla_\perp^2 j + \Omega\nabla_\parallel n_e \quad (2)$$

$$\frac{dU}{dt} = S^2(\nabla_\parallel j - \varepsilon\beta_e \frac{\partial n_e}{\partial z}) + \mu\nabla_\perp^2 U + \mathrm{S_m} \quad (3)$$

$$\frac{dv_\parallel}{dt} = -C_s^2\nabla_\parallel p / n_e + \mu\nabla_\perp^2 v_\parallel \quad (4)$$

Differing from Ref. [5], in Eqs. (1-4) the cold ion assumption is made, while the bootstrap current density, electron inertia and viscosity are taken into account in Ohm's law. The magnetic field $\boldsymbol{B}=[(B_{0t}+b_t)/R]\boldsymbol{e}_t+\nabla\psi\times\boldsymbol{e}_t$, where B_{0t} is the vacuum toroidal field, b_t is due to the diamagnetic correction, $\boldsymbol{e}_t$ is the unit vector along the toroidal direction, R the major radius, and ψ the flux function. The ion velocity $v=\boldsymbol{v}_{||}+\boldsymbol{v}_\perp$, the subscripts || and ⊥ denote the parallel and perpendicular components, $d/dt=\partial/\partial t+\boldsymbol{v}_\perp\cdot\nabla$, j and j_b are the toroidal plasma and bootstrap current density, $U=-(R/R_0)^2\nabla_\perp^2\phi$ the plasma vorticity, ϕ the stream function, n_e the electron density, $\varepsilon=a/R_0$ the inverse aspect ratio, R_0 the major radius of the magnetic axis, z the coordinate along the vertical direction, η the plasma resistivity, μ (μ_e) the ion (electron) viscosity, and D the particle diffusivity. S_n and S_m are the particle and momentum sources, E_0 is the equilibrium electric field, $S=\tau_R/\tau_A$, $p=p_e=n_eT_e$, $d_1=\omega_{ce}/\nu_{ei}$, $\Omega=\beta_e d_1$, $C_s=[T_e/m_i]^{1/2}/(a/\tau_R)$, $\beta_e=4\pi n_eT_e/B_{0t}^2$, T_e is the electron temperature, ω_{ce} the electron cyclotron frequency, υ_{ei} the electron-ion collisional frequency, $\tau_R=a^2/\eta$, $\tau_A=a/V_A$, and V_A is defined using B_{0t}.

2. Numerical results

The straight field line coordinate (r, θ, ζ) is utilized with the Jacobian $\sqrt{g}=rR^2/R_0$, where r is the minor radius of the equilibrium magnetic surface, and θ and ζ are the "poloidal-like" and toroidal angles [6]. In this coordinate system the operator $\boldsymbol{B}\cdot\nabla$ takes a simple form. The numerical code TM1.f has been upgraded to include the toroidal coupling among modes with the same toroidal mode number n but different poloidal mode number m, in addition to nonlinear two-fluid effects [7]. In our simulations the modes with the helicity m/n=1/1 and 3/2 as well as those due to their coupling are calculated simultaneously, focusing on the triggering of the m/n=3/2 modes by sawteeth.

The following plasma parameters, $B_{0t}=2T$, $a/R_0=0.5/1.7m$, $T_e=2keV$ and $n_e=3\times10^{19}m^{-3}$, are utilized, leading to $S=2.6\times10^8$ and $\nu_{ei}=2.2\times10^4/s$. Furthermore, $\mu_e/\upsilon_{ei}=10^{-4}a^2$, $\mu=0.2/m^2/s=19(a^2/\tau_R)$, $D_\perp=\mu/5$, and a monotonic profile for the safety factor q is assumed, with $q_0=0.91$ and $r_{q=1}=0.3a$, where q_0 is the original safety factor at $r=0$, and $r_{q=1}$ the minor radius at $q=1$ surface. The $q=3/2$ surface is at $r_{3/2}=0.68a$ with a local bootstrap current density fraction 0.18. Without coupling to the $m/n=2/2$ component, the $3/2$ mode is stable in the linear phase. The equilibrium magnetic surfaces are shifted circles with $n_e=n_{e0}[1-(r/a)^2]^2$.

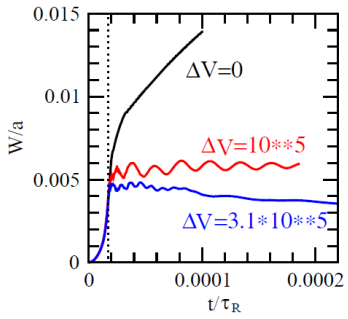

Figure 1 Time evolution of $W_{3/2}/a$ for $\Delta V=0$ (black), $10^5 a/\tau_R$ (red) and $3.1\times10^5\ a/\tau_R$ (blue).

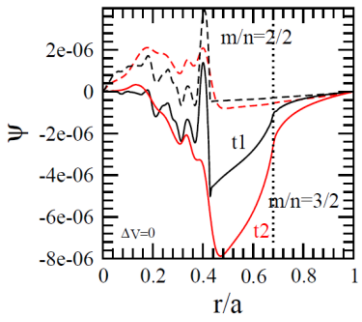

Figure 2 Radial profiles of $\psi_{3/2}$ (solid curve) and $\psi_{2/2}$ (dashed) at t_1 (black) and t_2 (red) for $\Delta V=0$.

Eqs. (1) - (3) correspond to the single fluid case for $\Omega=C_s=d_I=0$ [8]. We first study the onset of the $3/2$ mode due to sawtooth in this case. The time evolution of the normalized $3/2$ "island width", calculated from $W=4[\psi_{3/2}/(B_\theta q'/q)]^{1/2}$ at $r_{3/2}$, is shown in Fig. 1 for $\beta_e=0.005$ with different equilibrium plasma rotation speed, where q/q' is the magnetic shear length. The sawtooth collapse ends at the time $t=1.7\times10^{-5}\tau_R$ marked by the vertical dotted line. For $\Delta V=0$, where ΔV is the difference between the poloidal equilibrium plasma rotation speed at the $q=1$ and $3/2$ surfaces, the 3/2 mode continues to grow slowly after its initial fast growth driven by

the $m/n=2/2$ perturbation during the sawtooth collapse. For a sufficiently large relative rotation speed, $\Delta V=3.1\times10^{5}a/\tau_R$, the mode decays after its initial growth, as expected.

Fig. 2 shows the radial profiles of the normalized (to aB_{0t}) flux functions $\psi_{3/2}$ (solid curve) and $\psi_{2/2}$ (dashed) at two different times, $t_1=3.3\times10^{-5}\tau_R$ (black) and $t_2=10^{-4}\tau_R$ ~2ms (red), for $\Delta V=0$ and $\beta_e=0.005$. After the sawtooth collapse, the $m/n=2/2$ perturbations are mostly in the region $r<0.4a$ where $q\sim1$. The $\psi_{3/2}$ profiles have the feature of the tearing mode across the $q=3/2$ surface marked by the vertical dotted line.

The radial profiles of $\psi_{3/2}$ at $t_1=2\times10^{-5}\tau_R$ and $t_2=3.9\times10^{-5}\tau_R$ are shown in Fig. 3 for $\beta_e=0.005$ and $\Delta V=3.1\times10^{5}a/\tau_R$ (blue and green). The black and red curves are the same as those shown in Fig. 2 for $\Delta V=0$. With or without the rotation, the amplitude of $\psi_{3/2}$ after sawtooth collapse is about the same in the region inside the $q=3/2$ surface marked by the vertical dotted line. However, $\psi_{3/2}$ is nearly zero outside the q=3/2 surface for a sufficiently large value of ΔV, showing the shielding effect of relative plasma rotation.

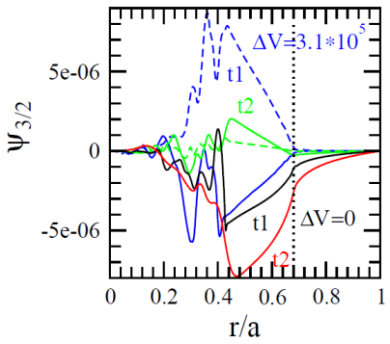

Figure 3 Radial profiles of $\psi_{3/2}$ at t_1 and t_2 for $\Delta V=0$ (black and red) and $3.1\times10^{5}a/\tau_R$ (blue and green). The solid (dashed) curves are real (imaginary) parts.

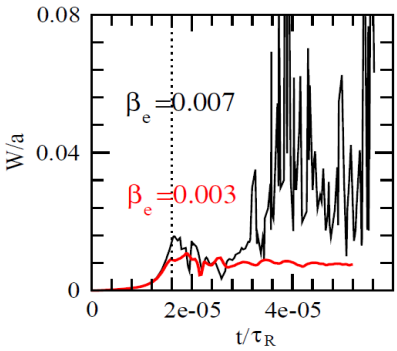

Figure 4 Time evolution of W/a for $\beta_e=0.007$ (black) and 0.003 (red). The sawtooth crash ends at t≈$1.6\times10^{-5}\tau_R$ marked by the vertical dotted line

When including the two-fluid effects with $\Delta V=0$, $\Omega=9.4\times10^{4}$, $C_s=2.0\times10^{7}(a/\tau_R)$ and $d_I=3.1\times10^{7}$, the time evolution of W/a is shown in Fig. 4 for $\beta_e=0.07$ (black curve) and 0.003 (red). Other parameters are kept unchanged in order to look into the effect of β_e. The toroidal coupling terms are explicitly proportional to β_e, as seen from Eqs. (1) and (3). After its initial growth during the sawtooth collapse, W decays for $\beta_e=0.003$ but continues to grow for $\beta_e=0.007$, showing the destabilizing effect of higher β_e value. The value of W oscillates in time right after its onset for $\beta_e=0.07$, being different from the single fluid case.

The radial profiles of the normalized flux functions $\psi_{3/2}$ at $t=5.6\times10^{-5}\tau_R$, corresponding to Fig.4, is shown in Fig. 5 for $\beta_e=0.007$ (black curve) and $\beta_e=0.003$ (red). For both cases the

values of $\psi_{3/2}$ does not vary smoothly across the q=3/2 surface marked by the vertical dotted line, indicating that the "constant ψ" assumption is not valid in this case. For a lower value of β_e, $\beta_e=0.003$, the amplitude of $\psi_{3/2}$ is much smaller.

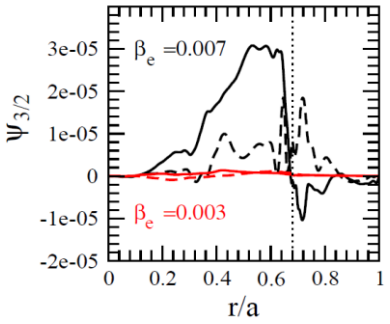

Figure 5 Radial profiles of $\psi_{3/2}$ at $t=5.6\times10^{-5}\tau_R$ for $\beta_e=0.007$ (black) and $\beta_e=0.003$ (red). The solid (dashed) curves are the real (imaginary) part.

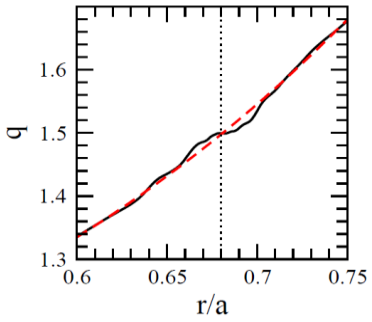

Figure 6 Radial profiles of the safety factor q (solid curve) for $\beta_e=0.007$ at $t=5.6\times10^{-5}\tau_R$. The dashed curve shows the original equilibrium one.

Corresponding to Fig. 5, the radial profile of the safety factor q is shown in Fig. 6 at $t=5.6\times10^{-5}\tau_R$. The q-profile is flattened across the q=3/2 surface during the mode onset when comparing to the original equilibrium one (dashed curve). In addition, the *m/n=0/0* component of the electron density is also found to be flattened around the q=3/2 surface, and the *m/n=0/0* component plasma rotation is generated, similar to the case without the *3/2* mode [7].

3. Summary

The triggering of the *m/n=3/2* mode by sawtooth collapse is studied numerically. For the single fluid case the onset threshold of the *3/2* mode is found to be affected by the difference between the plasma rotation speed at the *q=1* and *3/2* surfaces. For the two-fluid case, the *3/2* mode is triggered after the sawtooth collapse for a sufficiently high value of the plasma beta. Further calculations will be carried out in order to find out the effect of other input parameters on the *3/2* mode onset.

[1] Zohm H. et al 2001 Phys. Plasmas **8** 2009.
[2] Günter S. et al 2001 Phys. Rev. Lett. **87** 275001.
[3] Gude A., Günter S. and Sesnic S. et al 1999 Nucl. Fusion **39** 127.
[4] Igochine V. et al 2014 Phys. Plasmas **21** 110702.
[5] Hazeltine R. D. et al 1985 Phys Fluids **28** 2466.
[6] Grimm R. C., Greene J.M. and Johnson J. L. Methods in Computational Physics, edited by Killeen J. (Academic Press, New York, 1976), Vol. **16**, p. 253
[7] Yu Q., Günter S. and Lackner K. 2015 Nucl. Fusion **55** 113008.
[8] Strauss H. R. 1977 Phys. Fluids **20** 1354.